Reference 40

IEEE PHOTONICS TECHNOLOGY LETTERS, VOL. 17, NO. 1, JANUARY 2005

Tunable Narrow Linewidth All-Buried Heterostructure Ring Resonator Filters Using Vernier Effects

Seung June Choi, *Member, IEEE*, Zhen Peng, Qi Yang, Sang Jun Choi, and P. Daniel Dapkus, *Fellow, IEEE*

***Abstract*—Channel configurable optical filters are realized by using buried heterostructure semiconductor ring resonators. Two rings having slightly different radii are laterally coupled to bus waveguides in a cascaded manner, which affords free spectral range (FSR) expansion and channel configuration by Vernier effects. The effective FSR and spectral linewidth at resonance measured from a drop port are 10.2 and 0.017 nm, respectively, that corresponds to a finesse (F) of 600. By shifting the resonant wavelength of one of the resonators with free carrier injection, we demonstrate digital tuning filters where a distinct channel isolation of 15–20 dB is achieved with 0.68-nm spectral spacing.**

***Index Terms*—Buried heterostructure (BH), channel configurable filters, finesse, ring resonators, free carrier injection (FCI), free spectral range (FSR), spectral linewidth, Vernier effects.**

I. Introduction

BUS-COUPLED optical ring resonators are versatile components for wavelength filtering, multiplexing, switching, and modulating in photonic integrated circuits. Achieving narrow linewidth filters in semiconductor resonators has been problematic owing to the strength of surface scattering loss $\alpha_{\rm scat}$ for whispering gallery modes in circular resonators fabricated from high index materials. $\alpha_{\rm scat}$'s of 5–30 cm^{-1} have been reported from air-guided semiconductor microring add–drop filters [1]. Since $\alpha_{\rm scat}$ is proportional to $\Delta n^2 = n_{\rm wg}^2 - n_{\rm cl}^2$ where $n_{\rm wg}$ and $n_{\rm cl}$ are the refractive indexes of the waveguide core and the cladding materials, respectively [2], reduction of Δn^2 will reduce the scattering loss.

We have demonstrated buried heterostructure (BH) resonators [3], in which the InGaAsP ($n_{\rm wg} = 3.40$) ring and bus waveguides are completely buried with InP ($n_{\rm cl} = 3.17$). This technology in [3] leads to low optical losses due to the reduced Δn^2, which enables us to achieve coupling-limited Qs greater than 10^5 from a bus-coupled 200-μm radius microring resonator. The bending loss ($\alpha_{\rm bend}$) in circular waveguides is a concern owing to the relatively weak optical mode confinement. Therefore, large radii rings are utilized to suppress $\alpha_{\rm bend}$ in buried structures, at the expense of the free spectral range (FSR). In this letter, we present BH ring resonators using Vernier effects for FSR expansion and resonant wavelength tuning. Here, two rings having slightly different radii are laterally coupled to input–output (I/O) bus waveguides in a cascaded arrangement, which allows us to expand the FSR of the output spectra considerably via Vernier effects [4]–[6].

The utility of cascade-coupled rings using Vernier effects is its wide tuning functionality. By slightly shifting the resonant wavelength of one of the cascade-coupled resonators, we are able to digitally tune the resonant modes of the entire resonator system. Free carrier injection (FCI) is used to tune each resonance of a resonator, which needs only few milliampere for reasonable spectral shifts [7]. Since the spectral spacing for digital tuning is purely dependent on the FSRs of the cascade-coupled resonators, any spectral grid can be realized by adjusting the physical dimensions of the microrings.

II. Device Fabrication

The device fabrication process for channel configurable filters is similar to that of passive BH semiconductor ring resonators [3], except for several steps added to achieve FCIs into the resonators. We initiate the epitaxial growth by growing a 2-μm-thick lightly n-type doped ($\sim 3 \times 10^{17}$ cm^{-3}) InP buffer layer on a (001)-oriented n$^+$-InP substrate. A lattice-matched 0.4-μm-thick InGaAsP ($\lambda_{\rm WG} = 1.25$ μm) waveguide layer is grown on top of the buffer. A 0.1-μm-thick SiN$_x$ layer is deposited on the wafer, on which the cascade-coupled ring filter designs are photolithographically transferred. In the photomasks, the physical linewidths for rings and bus waveguides are designed as 0.9 and 0.8 μm, respectively, which ensures a single-mode operation, whereas, the end of the bus lines are gradually tapered wide to 4.5 μm to facilitate optical fiber coupling in measurements. Typical facet-to-fiber coupling losses are approximately -4 dB when a single-mode fiber with an antireflection (AR)-coated end is used. The lateral separation between the ring and the bus waveguides is 0.9 μm, from which 5%–7% of coupling efficiencies are predicted for the given materials [3]. Smooth and vertical 0.6-μm-deep waveguide mesas are dry-etched in a CH$_4$-based reactive ion etching discharge [8].

Once the resonator and bus waveguide mesas are defined, the SiN$_x$ mask material is removed by buffered oxide etchant (BOE). Then, a 0.6-μm-thick nominally undoped InP layer is overgrown to bury the dry-etched mesa structures and to minimize the overlap of the optical mode in the waveguide with the absorptive p-doped materials used in the top cladding. A 1-μm-thick p-type doped ($\sim 5 \times 10^{17}$ cm^{-3}) InP top cladding

Manuscript received July 8, 2004; revised August 19, 2004. This work was supported by the Defense Advanced Research Projects Agency under the Chip-Scale Wavelength Division Multiplexing Program.

S. J. Choi, Z. Peng, Q. Yang, and S. J. Choi are with the Department of Electrical Engineering-Electrophysics, University of Southern California, Los Angeles, CA 90089 USA (e-mail: seungjuc@usc.edu; zhenpeng@usc.edu; qyang@usc.edu; sangjunc@usc.edu).

P. D. Dapkus is with the Departments of Electrical Engineering and Materials Science, University of Southern California, Los Angeles, CA 90089-0243 USA (e-mail: dapkus@usc.edu).

Digital Object Identifier 10.1109/LPT.2004.838626

Report Documentation Page

Form Approved
OMB No. 0704-0188

1. REPORT DATE	2. REPORT TYPE	3. DATES COVERED
01 JUN 2005	**N/A**	**-**

4. TITLE AND SUBTITLE	5a. CONTRACT NUMBER
Tunable Narrow Linewidth All-Buried Heterostructure Ring Resonator Filters Using Vernier Effects	5b. GRANT NUMBER
	5c. PROGRAM ELEMENT NUMBER
6. AUTHOR(S)	5d. PROJECT NUMBER
	5e. TASK NUMBER
	5f. WORK UNIT NUMBER
7. PERFORMING ORGANIZATION NAME(S) AND ADDRESS(ES)	8. PERFORMING ORGANIZATION REPORT NUMBER
Department of Electrical Engineering-Electrophysics, University of Southern California, Los Angeles, CA 90089 USA	
9. SPONSORING/MONITORING AGENCY NAME(S) AND ADDRESS(ES)	10. SPONSOR/MONITOR'S ACRONYM(S)
	11. SPONSOR/MONITOR'S REPORT NUMBER(S)

12. DISTRIBUTION/AVAILABILITY STATEMENT
Approved for public release, distribution unlimited

13. SUPPLEMENTARY NOTES
See also ADM001923.

14. ABSTRACT

15. SUBJECT TERMS

16. SECURITY CLASSIFICATION OF:			17. LIMITATION OF ABSTRACT	18. NUMBER OF PAGES	19a. NAME OF RESPONSIBLE PERSON
a. REPORT	b. ABSTRACT	c. THIS PAGE			
unclassified	**unclassified**	**unclassified**	**UU**	**3**	

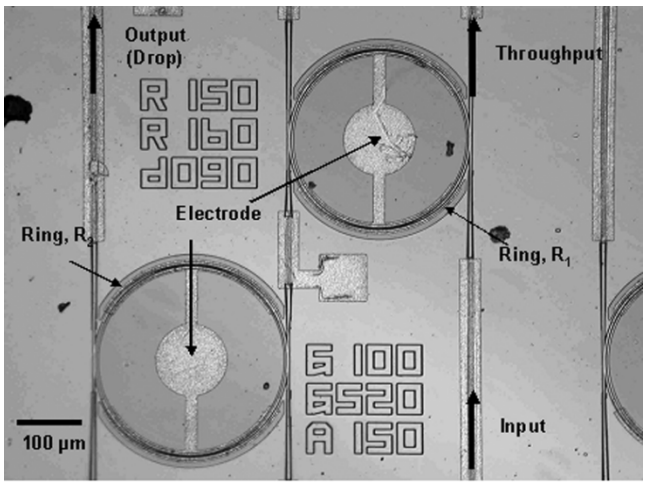

Fig. 1. Micrograph of the fabricated channel configurable filter using buried hetero-structure ring resonators.

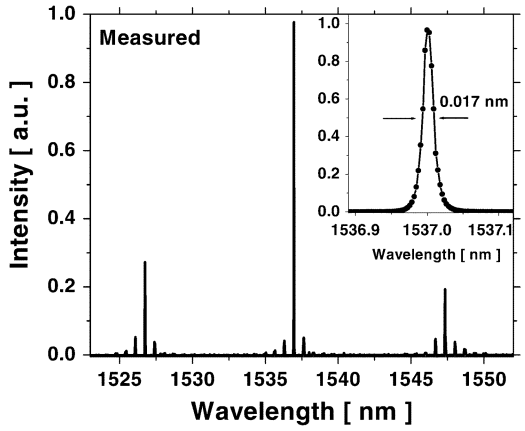

Fig. 2. Measured output spectrum of cascade-coupled ring resonators. In the inset, the resonant characteristics at 1537.0 nm are observed with high-resolution measurements.

layer and a 0.1-μm-thick p-InGaAs contact layer are grown to complete a p-i-n diode structure for current injection. Then, circular trenches approximately 1.5 μm deep are dry-etched for electrical isolation in the vicinity of the buried microrings, followed by p-and n-type ohmic electrode formation. Fig. 1 shows a top view of the fabricated device. After the wafer is mechanically thinned and cleaved for measurement, the cleaved waveguide facets are AR-coated to suppress unwanted Fabry–Pérot resonances.

III. Results and Discussions

The fabricated channel configurable filter (Fig. 1) is composed of two ring resonators having slightly different radii for Vernier effects. The rings are cascade-coupled through an intermittent bus waveguide, as shown in Fig. 1. The nominal radii of Resonators 1 (R_1) and 2 (R_2) are 150 and 160 μm, respectively. For the given material systems, the FSRs of $R_1(\mathrm{FSR}_{R1})$ and $R_2(\mathrm{FSR}_{R2})$ are expected to be 0.68 and 0.64 nm, respectively, in the spectral range of interest for transverse-electric (TE) polarization. Therefore, the resultant FSR in output is expanded by Vernier effects to $\sim$10.2 nm that is the least common multiple (LCM) of FSR_{R1} and FSR_{R2}. The optical resonant characteristics are measured by having a TE polarized external tunable laser source coupled into the input bus waveguide and collecting the dropped (transmitted) signals at the end of the output- (throughput-) bus line. Coupling of modes in space [9] and in time domain [10] formalisms are used to analyze the resonant behavior.

Since the second cascade-coupled resonator is not directly coupled to the throughput bus waveguide of the other resonator, it has no effect on its throughput transmission characteristics. Thus, the actual radius (r), the effective index (n_{eff}), the coupling coefficient between the ring and the bus waveguides (κ), and the optical loss (α) in each resonator can be experimentally measured in an independent manner by investigating the resonant transmission characteristics measured from a throughput waveguide. For TE polarization input, the measured radii (r_1/r_2), effective indexes $(n_{\mathrm{eff},R1}/n_{\mathrm{eff},R2})$, κ, and α are 150.8/160.5 μm, 3.302/3.313, 6%, and 0.6 cm^{-1}, respectively, at $\lambda = 1537$ nm. The n_{eff}, however, varies with wavelength. The $\mathrm{FSR}_{R1}(\mathrm{FSR}_{R2})$ measured from transmission spectra varies from 0.65 (0.63) to 0.69 (0.67) nm as λ is scanned from 1520 to 1560 nm, which indicates that the associated $n_{\mathrm{eff}R1}(n_{\mathrm{eff}R2})$ varies from 3.306 (3.316) to 3.298 (3.308) in the given spectral range. The transverse-magnetic (TM) polarization characteristics are similar after accounting for the slightly (1%) smaller effective index of the TM modes. Although the optical losses are reduced in the buried structures [3], the accumulated round-trip loss in the resonators L_{RT} is still as high as 5.7%, which results in the system being under-coupled (i.e., the input coupling coefficient is weak, compared to the sum of the output coupling and L_{RT}). The given parameters predict an insertion loss of -6 dB for the entire resonator block, which is consistent with the measured output intensity at near $\lambda = 1537$ nm. The origin of the optical losses observed in the waveguides has not been unambiguously identified. Nevertheless, since $\alpha_{\mathrm{scat}} < 0.1$ cm^{-1} and $\alpha_{\mathrm{bend}} < 0.1$ cm^{-1} are predicted from the given device configurations [3], the residual material losses in the nominally undoped waveguide as well as the absorption from the adjacent p- and n-doped layers would be considered as the primary loss mechanisms.

The measured drop port spectrum of cascade-coupled ring resonators is given in Fig. 2, where the input port is excited by an external tunable laser with TE polarization. We observe that Vernier effects have greatly expanded the effective FSR in the drop port from 0.65 to $\sim$10.2 nm, as was predicted. The measured spectral linewidth $(\Delta\lambda)$ of the resonance at $\lambda = 1537$ nm is 0.017 nm. The measured finesse $F = \mathrm{FSR}/\Delta\lambda$ is 600. If there were no wavelength dependence of the refractive index, a periodic set of resonant modes having identical intensities should appear in the output spectrum with a constant FSR that equals the LCM of FSR_{R1} and FSR_{R2}. However, the measured spectrum in Fig. 2 shows only one "primary" resonant mode at $\lambda = 1537$ nm over a wide spectral range, which suggests that the dispersion of refractive indexes must be taken into account for a more accurate data fitting process.

The final data fit is shown in Fig. 3, where the measured spectrum in Fig. 2 is nicely reproduced. Here, a linear model is employed to fit the chromatic dispersion of refractive indexes as provided in the inset of Fig. 3, whereas the weak dispersion of κ is neglected. The estimated dispersion $\Delta n_{\mathrm{eff}}/\Delta\lambda$ is approximately -0.0002 nm^{-1} for the given material systems,

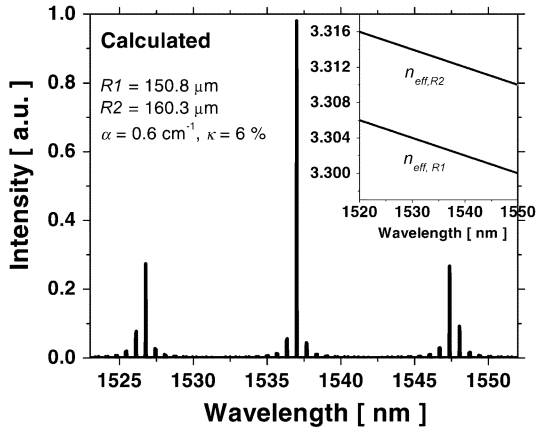

Fig. 3. Calculated output spectrum that reproduces the result given in Fig. 2. The dispersion of refractive indexes is given in the inset.

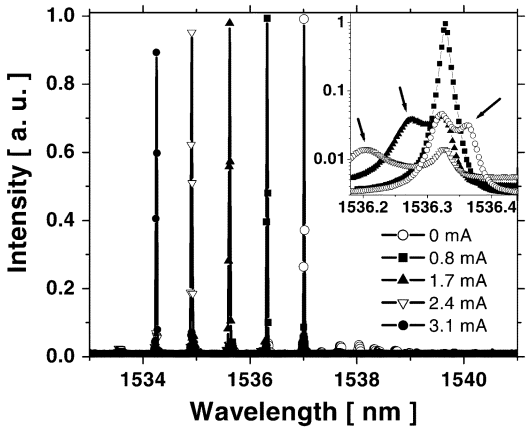

Fig. 4. Measured output spectra of a channel configurable filter, where the data measured at different current injection levels are superimposed. Free carriers are injected into Resonator 2 (R_2) to tune its resonant wavelength, by which the resultant resonance of the overall cascade-coupled ring system is digitally tuned with a spectral channel spacing of 0.68 nm. In the inset, the detailed resonant characteristics at 1536.32 nm are plotted on a logarithm scale.

which is consistent with the wavelength-dependent FSRs measured at throughputs. The effect of dispersion on the output spectra is more significant for very high-Q resonators than for lower Q structures due to the narrow spectral linewidth at each resonance. The as-fabricated primary resonance occurs at any wavelength where the resonant modes from R_1 and R_2 are at the closest coincidence. When it is desired to have the primary resonance appear at a specific wavelength, one of the resonators must be actively tuned to relocate its resonant spectra. Once the primary resonant mode is obtained as intended, the resonant wavelength of the entire filter system can be configured by subsequent tuning processes as described in the following paragraphs.

Digital tuning of resonant wavelengths of the fabricated devices is achieved by injecting free carriers into one of the cascade-coupled microring resonators. FCI blue-shifts the resonant wavelength of resonators in the spectral range of interest. Since there are two rings whose FSRs are not identical, different spectral channel spacings are possible in this digital tuning, depending on which resonator is chosen for FCI tuning. As a matter of fact, continuous analog tuning is also achievable when both resonators are tuned in a synchronized manner. In this experiment, we inject free carriers into R_2 only, so that a 0.68-nm spectral spacing (i.e., FSR_{R1}) is achieved for the digital tuning as presented in Fig. 4.

The inset in Fig. 4 shows the detailed resonant characteristics at near 1536.32 nm on a logarithmic scale. The superimposed spectra are measured at different injection levels on R_2, from which we can clearly observe FCI tuning mechanisms combined with Vernier effects. At $I = 0$ mA, the resonant modes of R_1 and R_2 coincide at 1537 nm, whereas, those at near 1536.32 nm are separated by $\sim$0.04 nm that corresponds to the difference in FSRs of the fabricated rings, $\Delta\mathrm{FSR}_{R1-R2} = \mathrm{FSR}_{R1} - \mathrm{FSR}_{R2}$. As the current injection level increases, the resonant modes of R_2 (indicated by arrows in the inset) are blue-shifted and the consequent resonant wavelength of the entire filter system is digitally tuned to the next channel at shorter wavelength. In Fig. 4, we observe that very narrow spectral linewidth ($<$0.02 nm) and distinct channel isolation ($>$17 dB) are maintained until the resonant wavelength is digitally tuned to 1534.28 nm at $I = 3.1$ mA. However, further increase of current injection results in degraded spectral linewidth and channel isolation for the following channels, due to free carrier absorption losses and thermal effects accompanying the FCI tuning. For instance, a degraded finesse of $F = 510$ is observed in the fifth channel at 1534.28 nm. Therefore, implementing gain in the resonator to offset these losses will be considered in future designs.

In conclusion, channel configurable high-Q Vernier filters are realized by using cascade-coupled BH semiconductor ring resonators. The effective FSR and spectral linewidth measured from a drop port are 10.2 and 0.017 nm, respectively, which corresponds to $F = 600$. By injecting free carriers into one of the ring resonators, we demonstrate channel configurable filters where a distinct channel isolation of 15–20 dB is achieved for over five consecutive optical channels with 0.68-nm spacing.

REFERENCES

[1] D. Rafizadeh, J. P. Zhang, R. C. Tiberio, and S. T. Ho, "Propagation loss measurements in semiconductor ring and disk resonators," *J. Lightw. Technol.*, vol. 16, no. 7, pp. 1308–1314, Jul. 1998.

[2] J. P. R. Lacey and F. P. Payne, "Radiation loss from planar waveguides with random wall imperfections," in *Proc. Inst. Elect. Eng. Optoelectronics Pt. J.*, vol. 137, Aug. 1990, pp. 282–288.

[3] S. J. Choi, K. D. Djordjev, Z. Peng, Q. Yang, S. J. Choi, and P. D. Dapkus, "Laterally coupled, buried heterostructure high-Q ring resonators," *IEEE Photon. Technol. Lett.*, vol. 16, no. 10, pp. 2266–2268, Oct. 2004.

[4] Y. Yanagase, S. Suzuki, Y. Kokubun, and S. T. Chu, "Box-like filter response and expansion of FSR by vertically triple coupled microring resonator filter," *J. Lightw. Technol.*, vol. 20, no. 8, pp. 1525–1529, Aug. 2002.

[5] S. T. Chu, B. E. Little, V. Van, J. V. Hryniewicz, P. P. Absil, F. G. Johnson, D. Gill, O. King, F. Seiferth, M. Trakalo, and J. Shanton, "Compact full C-band tunable filters for 50 GHz channel spacing based on high order micro-ring resonators," in *Proc. Optical Fiber Communication Conf.*, Los Angeles, CA, 2004, Postdeadline Paper 9.

[6] P. Rabiei and W. H. Steier, "Tunable polymer double micro-ring filters and modulators," *IEEE Photon. Technol. Lett.*, vol. 15, no. 9, pp. 1255–1257, Sep. 2003.

[7] K. D. Djordjev, S. J. Choi, S. J. Choi, and P. D. Dapkus, "Microdisk tunable resonant filters and switches," *IEEE Photon. Technol. Lett.*, vol. 14, no. 6, pp. 828–830, Jun. 2002.

[8] S. J. Choi, K. D. Djordjev, S. J. Choi, and P. D. Dapkus, "CH_4-based dry etching of high Q InP microdisks," *J. Vac. Sci. Technol. B*, vol. 20, pp. 301–305, Jan. 2002.

[9] H. A. Haus, *Waves and Fields in Optoelectronics*. Englewood Cliffs, NJ: Prentice-Hall, 1984.

[10] B. E. Little, S. T. Chu, H. A. Haus, J. Foresi, and J.-P. Laine, "Microring resonator channel dropping filters," *J. Lightw. Technol.*, vol. 15, no. 6, pp. 998–1005, Jun. 1997.